JOURNAL OF AIRCRAFT
Vol. 43, No. 1, January–February 2006

Drag Reduction on Gurney Flaps by Three-Dimensional Modifications

R. Meyer,* W. Hage,* and D. W. Bechert†
DLR, German Aerospace Center, D-10623 Berlin, Germany
and
M. Schatz‡ and F. Thiele§
Technical University Berlin, D-10623 Berlin, Germany

Miniflaps at the trailing edge of airfoils, that is, Gurney flaps, change the Kutta condition and thereby produce higher lift. Unfortunately, because of the flow separation downstream of such trailing edges, the drag also increases. Investigations are described with the aim to stabilize the wake flow to achieve drag reduction. When hot-wire anemometry is used, a tonal component in the spectrum of the velocity fluctuations downstream of the Gurney flap is shown. This points to the existence of a von Kármán vortex street. Modifications of the Gurney flap can reduce this flow instability, which results in a drag reduction. Trailing-edge modifications, such as slits or holes in Gurney flaps and vortex generators, were tested in experiments. The experiments were carried out using straight wings and a swept wing at a $Re = 1 \times 10^6$ At lower angles of attack of the airfoils with geometrical modifications a drag reduction was observed. This drag reduction was determined through force measurements. The flowfield behind the Gurney flaps was also investigated numerically, using methods based on Reynolds averaged Navier–Stokes and detached eddy simulation. The results confirm the existence of a two-dimensional vortex street as well as drag reduction by introducing slits in the Gurney flaps.

Nomenclature

C_D	=	drag coefficient
C_L	=	lift coefficient
$C_{L\,\max}$	=	maximum lift coefficient
C'_L	=	lift coefficient gradient
c	=	chord length
f_0	=	discrete frequency
h	=	trailing edge height
h_{GF}	=	Gurney flap height
h/c	=	ratio of Gurney flap height to chord length
Re	=	Reynolds number
S_{ij}	=	mean flow strain rate tensor
Sr	=	Strouhal number
u'	=	velocity fluctuation
$\bar{u}$	=	mean velocity
y	=	vertical coordinate
α	=	angle of attack
Δh_{GF}	=	effective Gurney flap height
$\varepsilon_{\max}$	=	maximum ratio of lift to drag
ε_n	=	maximum residual in mass and momentum balance normalized by global mass flux
λ_2	=	second eigenvalue of the vorticity tensor
φ	=	sweep angle
Ω_{ij}	=	mean flow rotation rate tensor

Received 28 October 2004; revision received 24 March 2005; accepted for publication 24 March 2005.

*Scientist, Department of Turbulence Research, Müller-Breslau-Straße 8.
†Group Leader, Department of Turbulence Research, Müller-Breslau-Straße 8. Senior Member AIAA. (Deceased.)
‡Scientist, Herrmann Föttinger Institute for Fluid Mechanics, Müller-Breslau-Straße 8. Member AIAA.
§Professor, Herrmann Föttinger Institute for Fluid Mechanics, Müller-Breslau-Straße 8. Member AIAA.

I. Introduction

THE necessity of increasing the lift of airplane wings for landing and takeoff has for many years been addressed by developing suitable flap systems. Split flaps were first developed and flown as early as 1930.[1] Particularly at high lift coefficients, split flaps are superior to simple flaps.[2] The high-lift systems of today's airliners are, however, substantially more complex and exhibit retractable slats and slotted flaps (Fowler flaps). Even more effective than split flaps, where the fulcrum lies in front of the trailing edge, are strongly deflected small flaps (up to 90 deg) having a fulcrum at the trailing edge. This configuration was described first by Zaparka[3] in a patent from 1935. A distinct lift increase is attained even with very small flaps of just 1% of the airfoil chord length. At the end of the 1960s, the racing driver and engineer Daniel Gurney installed small fixed flaps of this kind on his vehicles (Gurney flaps). Nowadays, they are used on all racing cars with wings producing downward force to improve road grip. Liebeck[4] realized the potential of this invention for airplane wings. Even with conventional flap/slat configurations, which have reached maximum performance with such designs, a further lift increase can be achieved by the additional mounting of a Gurney flap.[5,6] The Gurney flap is a fairly inconspicuous small trailing-edge modification with typical dimensions of only approximately 1% of the airfoil chord length. A further example of a trailing-edge modification is the so-called diverging trailing edge on transonic airliner airfoils. In this, the work of Henne[7] particularly may be regarded as pioneering. In the meantime, this concept has been developed further up to application on airliners (McDonnell Douglas MD 11). After the acquisition of McDonnell–Douglas by The Boeing Company, divergent trailing edges were also successfully tested on a Boeing 747.[8] With a Gurney flap, the aerodynamic loading of the lower surface of the wing is increased for the same overall lift, the upper surface being thereby relieved.[9–11] As a consequence, the local supersonic Mach number on the forward part of the upper side of the airfoil is lower. This ensures weaker shock at the downstream end of that supersonic flow region and the drag is significantly reduced.[7,9,10] However, the design of such profiles is not trivial because a blunt trailing edge per se causes an increase of drag. Nevertheless, for transonic airliner airfoils, modified trailing edges are evidently an interesting possibility for improvements. Further important applications of modified airfoil trailing edges can

be seen with fluid flow machines. An increase in the output of wind turbines has already been reached using Gurney flaps.[12] The noise generation by wind turbines is particularly critical, and the separated unstable flow behind a Gurney flap does contribute unfavorably to noise generation.

First computations of the flow around a Gurney flap have been published by Sauvage[11,13] and produce qualitatively useful predictions of the time-averaged flow situation. Further computational investigations that also refer only to mean quantities were done by Lee and Kroo.[14] A more detailed time-resolved numerical study of the unsteady flow has been published recently.[15] The results indicated the appearance of a two-dimensional von Kármán vortex street in the wake of the Gurney flap also coupled with lift fluctuations. Such behavior is well known in the wake of bluff bodies.[16] Hot-wire measurements conducted in the wake of a Gurney flap also confirmed this.[17,18]

In the literature, however, only few references to this phenomenon are to be found.[19] Stabilization of the wake behind cylinders or bluff bodies, and thus an elimination of the von Kármán vortex street, can be achieved using splitter plates. These are thin plates, which are introduced into the wake flow. When splitter plates are used, a clear drag reduction can be achieved in the case of cylinders.[20] The potential benefits of using splitter plates behind Gurney flaps are obvious. In the study by Sauvage,[11] the flow around a very short splitter plate is computed, albeit with an inappropriate method based only on stationary quantities. Furthermore, the application of a splitter plate behind a diverging trailing edge for the purpose of drag reduction is explicitly described in the patent specification of Allen.[21]

Altogether, the insights into the interaction between wake instability and drag reduction are rather rudimentary in the existing literature. Our present research, therefore, aims to address this issue.

II. Experimental Setup

A. Wind-Tunnel Experiments with a Force Balance

Two different straight wings were investigated in the two-dimensional airfoil test section of a wind tunnel (Fig. 1). The test section has a diameter of 1.4×2.0 m. The maximum airspeed is 40 m/s. The turbulence intensity in the wind tunnel is less than 0.1–0.2%. The tested wing is connected to the wind-tunnel balance, thereby permitting a direct force measurement of the overall air loads acting on the wing (lift, drag, and pitching moment). The initial gap of 2 mm between the wing and the side wall is reduced to 0.1 mm during the measurements with a thin adhesive tape. The angle of attack is adjusted by a stepping motor operated gear with an accuracy of 0.1 deg. At the airfoil, an essentially two-dimensional flow is obtained.

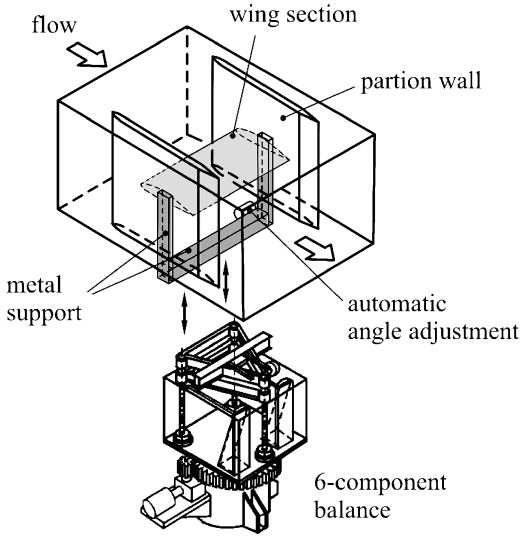

Fig. 1 Wind-tunnel test section with two-dimensional wing model.

The two-dimensional flow quality was checked by flow visualizations. Here, 85% of the wing span is completely two-dimensional. The other 15% is influenced by the turbulent boundary layer of the sidewalls. The measured drag with the force balance is slightly higher then that of the plain wing section drag due to induced drag components of the gap and due to the turbulent boundary layer at the side walls. The force balance has an accuracy of 0.2% for the lift and drag components. A more detailed description of the two-dimensional test section and the wind tunnel is published in Ref. 22.

B. Test Model Description

Two wings with a span of 1.55 m, with a chord length of 0.50 m, and with different airfoil cross sections (Fig. 2) were investigated. The airfoils have a characteristic trailing-edge thickness of $h/c = 0.33\%$. The first wing exhibits a typical laminar glider profile HQ17/14.38, with a minimal drag at moderate angles of incidence, for example, at cruise condition. The profile was developed by Horstmann and Quast from DLR, German Aerospace Center, Brunswick. This wing is particularly suitable for measurements of the smallest drag changes arising from the trailing-edge modifications. The maximum lift coefficient of this airfoil is $C_{L\max} = 1.4$. The second wing is the high lift airfoil (FX73-CL3-152) devised by Wortmann, which has a strong curvature and achieves a very high maximum lift coefficient of $C_{L\max} = 2.2$. The indicated $C_{L\max}$ values refer to an airfoil Reynolds number of $Re = 1 \times 10^6$. In addition to extensive investigations with the two-dimensional test section, measurements on a swept wing with one free wing tip were carried out.

A simplified swept constant chord half (SCCH) model with a typical modern airliner airfoil was fitted to the wind-tunnel force balance (Fig. 3). This model consists of a swept wing $\varphi = 30$ deg, of half-span of 1.12 m and constant chord of 0.45 m, a half-cylindrical fuselage, and a boundary-layer base. The drag and lift on the boundary-layer base is not measured and not contained in the data. A more detailed description of this test section is published in Ref. 22. With this model, investigations of different wing configurations (clean for cruise and high-lift configurations for start and landing) can be carried out.

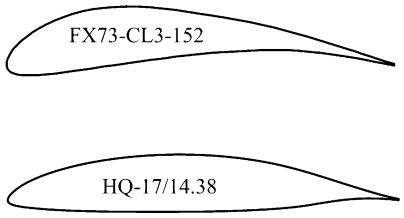

Fig. 2 Investigated airfoils.

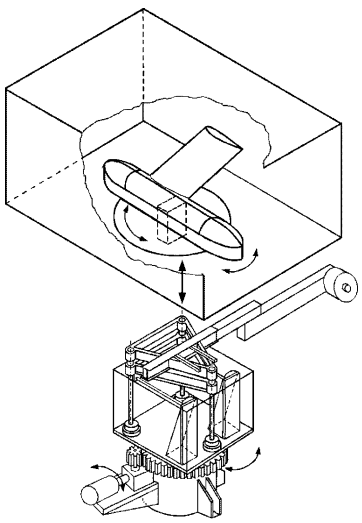

Fig. 3 Wind tunnel test section with SCCH model mounted on under-floor six components balance.

III. Drag Reduction by Wake Stabilization

In the separated flow downstream of a Gurney flap, we expect that an absolute instability[23–25] can be observed. One well-known example of an absolute instability is the von Kármán vortex street, which occurs in the wake of a cylinder. Such instabilities occur not only in laminar flows, as the classical experiments with cylinders would suggest, but they also can be observed in turbulent flows. A telltale sign for an absolute instability is the occurrence of a single peak in the spectrum of the fluctuations in or near the wake. The reversed flow in the wake is a property that enhances this instability.[24] Because trailing edges of airfoils are seldom very sharp, we also expect such an absolute instability in the wake of an (even slightly) blunt trailing edge.

Our first aim is, therefore, to demonstrate experimentally that a single frequency does exist in the fluctuations downstream of the trailing edge and then devise trailing-edge modifications to suppress those periodic fluctuations. The easiest way to measure velocity fluctuations is provided by the well-established hot-wire anemometry (Fig. 4). The anemometer output signals were plotted to obtain the mean flow distribution downstream of the wing. In places of maximum mean velocity gradient, the highest streamwise velocity fluctuations u' occurred. The u' fluctuations were collected at two locations with steep mean flow velocity gradient (Fig. 5). The u' fluctuation signals were Fourier-analyzed, and the spectra were plotted. Figure 6 shows recorded data of the reference wing without Gurney flap. Because of the finite thickness of the trailing edge (0.33% chord) of this wing, there is a small hump in the spectrum, signifying an (albeit weak) absolute instability, which is highlighted by its single resonance frequency $f_0 = 2.4$ kHz. By the way, this hump vanishes for a very sharp trailing edge.

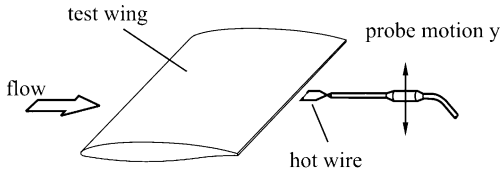

Fig. 4 Test arrangement for wake measurements with a hot wire.

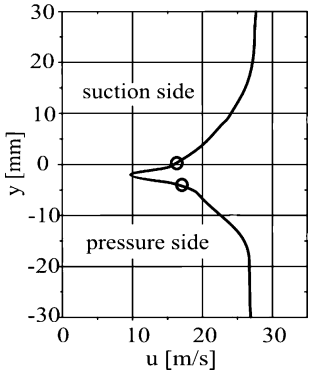

Fig. 5 Mean flow $\bar{u}$ distribution of wake, airfoil HQ17, $\alpha = -1$ deg, and $Re = 1.0 \times 10^6$: ○, position of u' data aquisition.

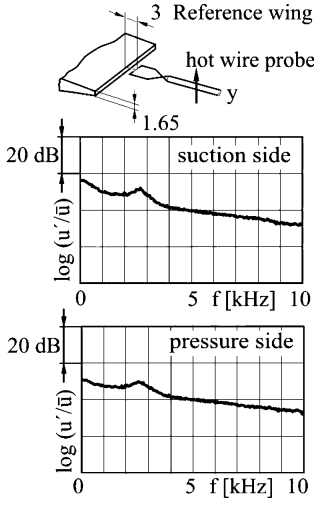

Fig. 6 Spectra of u' fluctuation of airfoil HQ17 with finite trailing edge (0.33% c); dimensions in millimeters, $\alpha = -1$ deg, and $Re = 1.0 \times 10^6$.

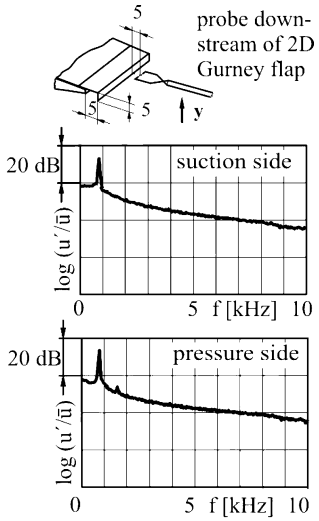

Fig. 7 Spectra of u' fluctuation in the wake of two-dimensional Gurney flap with a total height of 1% c: airfoil HQ17, $Re = 1.0 \times 10^6$, and $\alpha = -1$ deg.

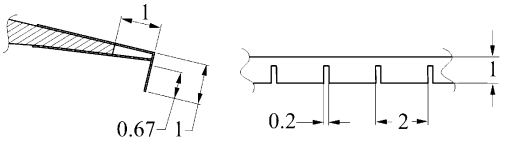

Fig. 8 Gurney flap and slit geometry, dimensions in percent chord.

The Gurney flap height that was used throughout the investigations has a total height of $h_{GF}/c = 1\%$, with an effective height of $\Delta h_{GF} = 0.67\%$, taking into account that the bluff trailing edge of the reference wing has a height of $h/c = 0.33\%$. The wake of a two-dimensional Gurney flap is wider, indicating a higher drag. In addition, the u' fluctuation levels are higher and the periodic constituent with the frequency $f_0 = 0.8$ kHz is much stronger (Fig. 7). The data are recorded at $Re = 1 \times 10^6$. Similar data are obtained if the mean flow velocity is reduced to one-half of its previous value, yielding a Reynolds number of 0.5×10^6. As expected, the peak frequency f_0 is also reduced to half of its previous value. If one calculates a Strouhal number with the frequency f_0, the Gurney flap height and the mean flow velocity, one obtains a resonance Strouhal number of $Sr \approx 0.14$. It is conceivable that other reference lengths, such as, for example, the momentum loss boundary layer (or wake) thickness, may be a more appropriate reference length here.

A. Gurney Flaps with Slits

It is known from the von Kármán vortex street on cylinders that a three-dimensional structure of the wake flowfield effectively suppresses the absolute instability. On a cylinder, that can be achieved by applying a helical structure on its surface, that is, the Screwton spiral, which can be seen quite often on industrial chimneys. Obviously, the same approach cannot be literally transferred to our problem. However, as it will turn out, there are various possibilities to obtain a three-dimensional wake flowfield.

First we consider the application of slits to the Gurney flaps (Fig. 8). The effect of slits on the wake can be seen in Figs. 9 and 10. The hot-wire data show clearly that the absolute wake instability, that is, the peak in the spectrum, has almost completely vanished. Drag polars can be seen in Figs. 11 and 12, and performance data are listed in Tables 1 and 2. It is obvious that the additional device drag is considerably decreased by 25%. On the other hand, the bleed air through the slits causes the Gurney flap to appear smaller, which slightly decreases the gain in lift. At higher angles of attack, however, the improvement due to the slits in the flaps is less pronounced. The hot-wire data of the two-dimensional Gurney flap (not shown here) do not exhibit any resonance either. As a matter of fact,

Table 1 Performance data of the Gurney flap with slits: airfoil HQ17, $Re = 1.0 \times 10^6$

Configuration	$C_{L\max}$	$C_{D\min}$	$\varepsilon_{\max}$
Reference wing, □	1.438	0.011	69.6
Two-dimensional Gurney flap, ○	1.627	0.015	63.6
Three-dimensional Gurney flap with slits, △	1.605	0.014	64.6

Table 2 Performance data of the Gurney flap with slits: airfoil FX73, $Re = 1.0 \times 10^6$

Configuration	$C_{L\max}$	$C_{D\min}$	$\varepsilon_{\max}$
Reference wing, □	2.272	0.017	61.8
Two-dimensional Gurney flap, ○	2.531	0.022	56.4
Three-dimensional Gurney flap with slit, △	2.505	0.021	56.9

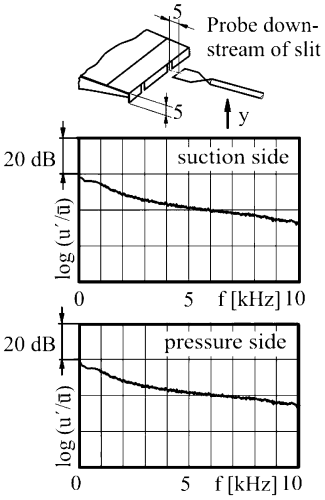

Fig. 9 Spectra of u' fluctuation downstream of slit in three-dimensional Gurney flap ($h_{GF}/c = 1\%$): airfoil HQ17, $Re = 1 \times 10^6$, and $\alpha = -1$ deg; dimensions in millimeters.

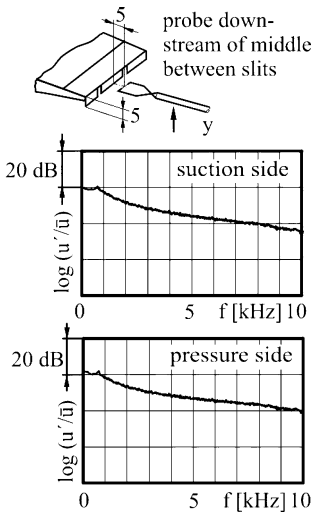

Fig. 10 Spectra of u' fluctuation downstream of middle between slits in three-dimensional Gurney flap ($h_{GF}/c = 1\%$): airfoil HQ17, $Re = 1 \times 10^6$, and $\alpha = -1$ deg; dimensions in millimeters.

Koch[25] has already predicted that the absolute instability disappears for strongly asymmetric wakes. Obviously, for high angles of attack, the wake of an airfoil becomes strongly asymmetric.

Therefore, one cannot reduce anymore the drag at high angles of attack by instability suppression in the wake. On the other hand, drag reduction is particularly desired at low angles of attack and, as Figs. 11 and 12 show, it is indeed achieved there. Finally, we expect that, due to the elimination of the absolute instability of the wake, also induced mechanical vibrations of the wing and radiated noise are very likely to be reduced.

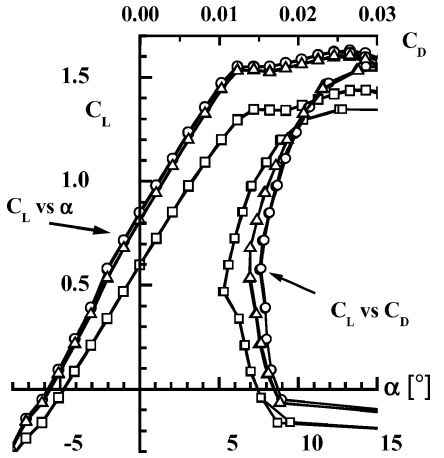

Fig. 11 Polar diagrams of airfoil HQ17 with Gurney flap with slits; $Re = 1.0 \times 10^6$ and $h_{GF} = 1\%$ c: □, reference wing; ○, two-dimensional Gurney flap; and △, Gurney flap with slits.

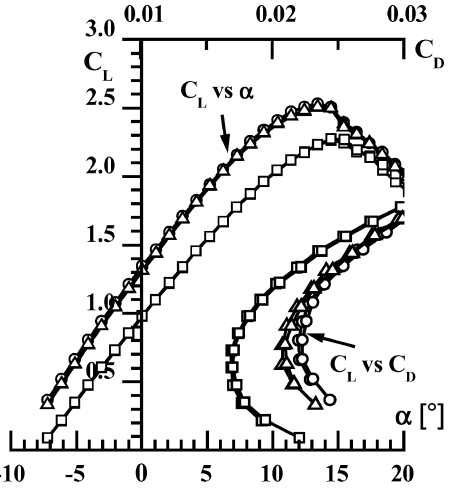

Fig. 12 Polar diagrams of airfoil FX73 with Gurney flap with slits; $Re = 1.0 \times 10^6$ and $h_{GF} = 1\%$ c: □, reference wing; ○, two-dimensional Gurney flap; and △, Gurney flap with slits.

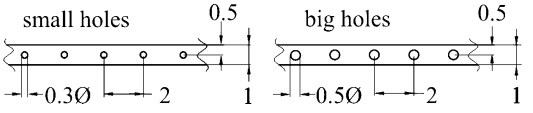

Fig. 13 Geometry of Gurney flap with holes, dimensions in percent chord.

B. Gurney Flaps with Holes

One disadvantage of having slits in the Gurney flap is that the additional mechanical stiffness of the trailing edge with Gurney flap is no longer available. Based on the idea that the reversed flow in the wake[11] is of crucial importance for the existence of an absolute instability,[24] we considered holes in the Gurney flap as an alternative. This has the advantage that the mechanical stiffness and stability of the Gurney flap is basically maintained. We have carried out tests with two sizes of holes, 0.3% chord and 0.5% chord in diameter (Fig. 13).

As Figs. 14 and 15 show, both are effective. Performance data are listed in Tables 3 and 4. The smaller holes draw less bleed air and thus cause lower losses in lift. The same data as with the smaller holes are obtained if the bigger holes are placed at double the lateral spacing. According to our hot-wire data (not shown here), the elimination of the wake instability is not as complete as with the slits, but it is significant enough to cause an equivalent drag reduction.

Table 3 Performance data of Gurney flap with holes: airfoil HQ17, $Re = 1.0 \times 10^6$

Configuration	$C_{L\max}$	$C_{D\min}$	$\varepsilon_{\max}$
Reference wing, □	1.438	0.010	69.6
Two-dimensional Gurney flap, ○	1.627	0.015	63.6
Gurney flap with small holes, △	1.611	0.014	65.4
Gurney flap with big holes, ▽	1.599	0.014	65.6

Table 4 Performance data of Gurney flap with holes: airfoil FX-73, $Re = 1.0 \times 10^6$

Configuration	$C_{L\max}$	$C_{D\min}$	$\varepsilon_{\max}$
Reference wing, □	2.272	0.017	61.8
Two-dimensional Gurney flap, ○	2.531	0.022	56.4
Gurney flap with big holes, △	2.510	0.021	56.8
Gurney flap with small holes, ▽	2.516	0.021	56.8

Table 5 Performance data of the Gurney flap with vortex generators: airfoil HQ17, $Re = 1.0 \times 10^6$

Configuration	$C_{L\max}$	$C_{D\min}$	$\varepsilon_{\max}$
Reference wing, □	1.438	0.010	69.6
Two-dimensional Gurney flap, ○	1.627	0.015	63.6
Gurney flap with vortex generators, ▽	1.62	0.014	63.5

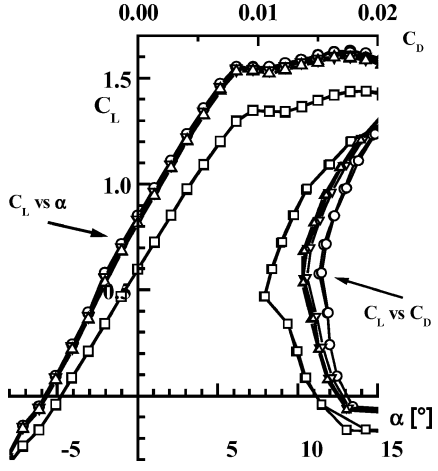

Fig. 14 Polar diagrams of airfoil HQ17 with Gurney flap with holes of different diameters: $Re = 1.0 \times 10^6$ and $h_{GF} = 1\%\ c$: □, reference wing; ○, two-dimensional Gurney flap; ▽, Gurney flap with small holes; and △, Gurney flap with big holes.

C. Gurney Flaps with Vortex Generators

Vortex generators can also be used to disturb the periodic flowfield in the wake of the two-dimensional Gurney flaps. In Fig. 16, the geometry of the vortex generators used on the Gurney flap is shown. The idea for the design of the vortex generators derives from the three-dimensional structure on the trailing edges of dragonflies. A more detailed description of these structures is published by the authors.[17]

Because of the vortex generators that are attached to the upper and lower surface of the Gurney flap, the wake of the Gurney flap is disturbed in such a manner that periodic separation should no longer occur. The disturbance by the vortex generators is introduced at the upper and lower edge of the Gurney flap and not in the center as with the holes and slits. The drag polar presented in Fig. 17 show the extent to which vortex generators reduce the parasitic drag of the Gurney flaps. Table 5 lists the performance data. The drag reduction is somewhat smaller than that of the Gurney flap with slits or holes.

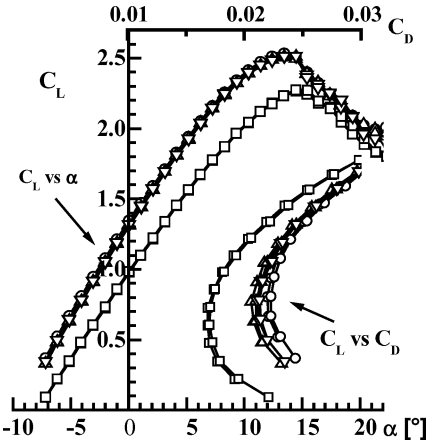

Fig. 15 FX-73 airfoil with Gurney flaps with holes of different diameters: $Re = 1.0 \times 10^6$ and $h_{GF} = 1\%\ c$: □, reference wing; ○, two-dimensional Gurney flap; △, Gurney flap with big holes; and ▽, Gurney flap with small holes.

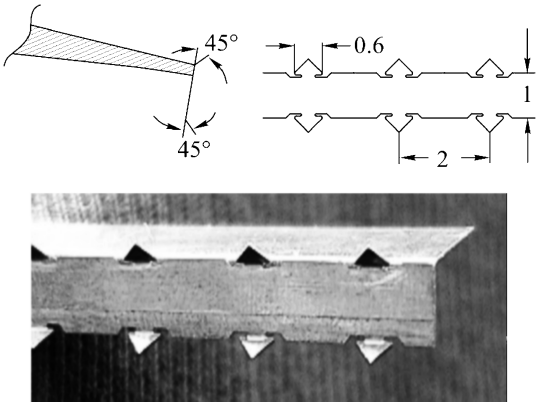

Fig. 16 Geometry of the Gurney flap with vortex generators.

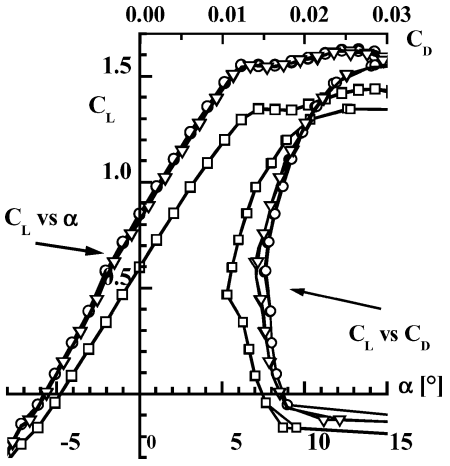

Fig. 17 Airfoil HQ17 with Gurney flap and vortex generators on the upper and lower edge of the Gurney flap: $Re = 1.0 \times 10^6$ and $h_{GF} = 1\%\ c$: □, reference wing; ○, two-dimensional Gurney flap; and ▽, Gurney flap with vortex generators.

D. Gurney Flaps with Slits on a Swept Wing

On the swept wing SCCH model, the three-dimensional Gurney flap with slits produces a drag reduction of 29% as compared to the two-dimensional Gurney flap at small angles of attack ($\alpha < 2.5$ deg) (Fig. 18). The data contain the forces on the half-fuselage, but not on the boundary-layer base. For angles of attack larger than $\alpha = 2.5$ deg, however, no difference in the drag behavior can be determined. This behavior can be explained on the basis of the hot-wire measurements. These were taken in the wake of the SCCH wing in the clean

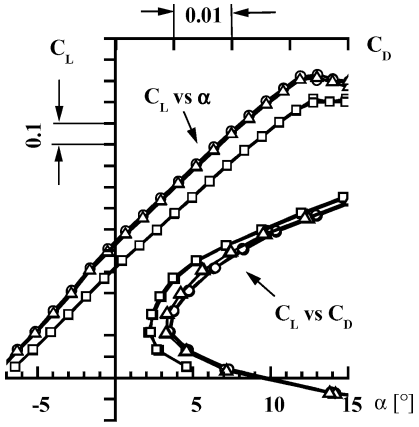

Fig. 18 SCCH model with two- and three-dimensional Gurney flaps with slits: $Re = 1.0 \times 10^6$ and $h_{GF} = 1.1\%\ c$: □, reference wing; ○, two-dimensional Gurney flap; and △, Gurney flap with slits.

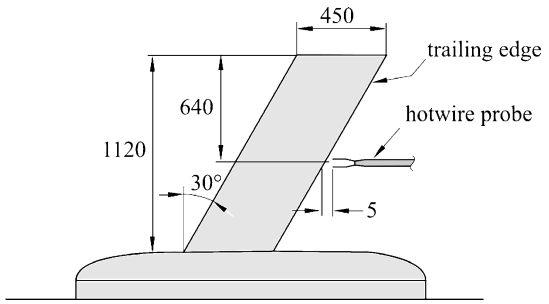

Fig. 19 Position of hot-wire probe relative to swept wing model, dimensions in millimeters.

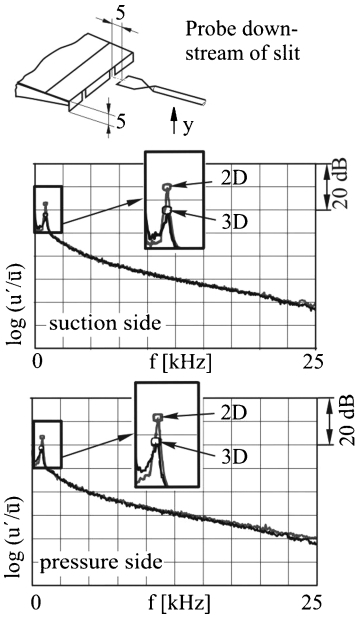

Fig. 20 Fluctuation spectra u' of SCCH model with three-dimensional Gurney flap $h_{GF} = 1.1\%\ c$, probe downstream of a slit; $\alpha = -1$ deg, $Re = 1.0 \times 10^6$; dimensions in millimeters.

configuration at a distance of 5-mm downstream of the Gurney flap (Fig. 19). At $\alpha = -1$ deg, the velocity distribution in the wake behind the wing of the SCCH model shows a similar boundary-layer thickness at the upper and lower surfaces of the airfoil. This is a requirement for the formation of an absolute instability.[23] In the shear layer, where the largest velocity gradients are found, the velocity fluctuations u' were measured and the corresponding spectra computed (Figs. 20 and 21). In the case of the two-dimensional Gurney flap, a discrete frequency in the spectrum is recognized as indication for an instability at 937 Hz. The corresponding Strouhal number calculated with reference to the height of the Gurney flap is $Sr = 0.16$.

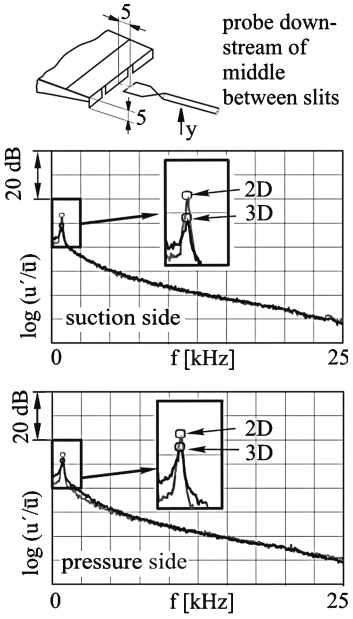

Fig. 21 Fluctuation spectra u' of SCCH model with three-dimensional Gurney flap $h_{GF} = 1.1\%\ c$: probe downstream of middle between slits, $\alpha = -1$ deg, $Re = 1.0 \times 10^6$; dimensions in millimeters.

This agrees well with the results of accompanying numerical investigations. The hot-wire measurements were conducted exactly behind the slit (Fig. 20) as well as between two slits (Fig. 21). In both cases, the discrete frequency is clearly reduced. The velocity distribution in the wake behind the SCCH model wing at $\alpha = 2.5$ deg is highly asymmetrical due to the different boundary-layer thicknesses on the suction and pressure sides of the wing. As expected, no discrete frequency can be found for this case in the spectrum of the velocity fluctuations u' because no periodic flow structures can develop in the wake.[25] The drag-decreasing effect of a three-dimensional Gurney flap is, therefore, no longer effective at such angles of attack.

IV. Numerical Simulation

The unsteady flow structures in the wake are additionally investigated by numerical simulations to understand the details of the flow physics better. The applied numerical method is based on a three-dimensional incompressible finite volume scheme to solve the Navier–Stokes equations. The method is fully implicit and of second order in space and time. Based on the semi-implicit method for pressure linked equations (SIMPLE), a collocated storage arrangement for all quantities is applied. Convective fluxes are approximated by a third-order total variation diminishing (TVD) monotonic upstream scheme for conservation laws (MUSCL) scheme. In the unsteady Reynolds-averaged Navier–Stokes (URANS) investigations, the linear local realizable (LLR) k–ω model by Rung[26] is used, which showed improved predictions of unsteady airfoil flows with large separation in former investigations.[27] Additionally, detached eddy simulations (DES) have been performed, which are also based on the LLR k–ω model; for details, see Ref. 15. The DES approach offers the possibility to yield results of high resolution and physical quality with much lower numerical effort than required by large-eddy simulations (LES).

The three-dimensional mesh around the HQ17 airfoil with a $h_{GF}/c = 1\%$ Gurney flap consists of 40 layers of an originally two-dimensional mesh with 453×89 cells covering $2h_{GF}$ in the spanwise direction and has about 1.6×10^6 nodes. The computational domain covers 7 chords upstream and 10 chords downstream of the configuration. The Gurney flap is represented by a single mesh line on both sides of which no-slip boundary conditions are applied. For the DES, the same three-dimensional mesh can be applied. Further investigations cover Gurney flaps with slits that can be compared to those discussed earlier (Fig. 8). The same mesh can be used for two-dimensional Gurney flaps, as well as for those with slits by removing the wall boundary condition on appropriate parts of the Gurney flap to create slits. The transition positions are fixed on the

suction and on the pressure sides of the airfoil. A separate study of the influence of time stepping indicated that a typical time step of $\Delta t = 0.002c/u$ is sufficient to obtain results independent of the temporal resolution and, thus, was used for both URANS and DES computations. At each single time step, the mass and momentum balances are solved until a residual of $\varepsilon_n < 10^{-6}$ normalized by the global mass flux is reached.

A. Two-Dimensional Gurney Flaps

Numerical simulations of the two-dimensional Gurney flap result in an almost completely two-dimensional flowfield and, therefore, at first two-dimensional URANS simulations were performed. Here, the mean lift clearly increases with the height of the Gurney flap. The relation between flap height and lift, however, is not linear but reaches saturation for very large Gurney flaps. The computational results show the same behavior that was observed in the experiments before, not only for the linear part of the polar but also for higher angles of attack. Comparisons between steady and unsteady numerical simulations indicate that the lift coefficient can be predicted accurately based on steady computations, whereas reliable results for the drag can only be obtained from unsteady computations.[15] Only these are able to capture the dynamics of flow structures in the wake, which play an important role for the drag.

For low angles of attack, the flow structures are much more clearly evident than at higher incidence, where interaction with other separation processes is dominating. Therefore, investigations are focused on a case with $\alpha = 0$ deg. Analysis of the time-depending lift coefficient shows that it can be characterized by one dominant frequency corresponding to the vortex shedding for all investigated cases. Table 6 lists the Strouhal number, which represents the dominant shedding frequency normalized by the flap height. The fluctuation intensity C'_L is based on the rms value of the lift coefficient. The characteristic behavior of the predicted frequencies is similar to those measured by hot-wire anemometry,[28] where increasing flap heights the frequency decreases. At the same time, however, the experimental Strouhal number increases and asymptotically reaches $Sr \approx 0.18$ for very large Gurney flaps, $h_{GF}/c > 5\%$. Compared to the hot-wire measurements (Fig. 7) and the experiments by the authors and by Zerihan and Zhang[28] reporting $Sr = 0.14$ for $h_{GF}/c = 1\%$, the Strouhal number is underestimated in the computations ($Sr = 0.11$). In the case of the clean airfoil and for the smallest Gurney flap, $h_{GF}/c = 0.5\%$, almost no unsteadiness can be identified in the lift coefficient and C'_L remains negligible. For larger flaps, the lift fluctuations become more eminent and grow larger proportionally to the flap height in a similar manner to the extra drag induced by the Gurney flap. This behavior is an indication that the intensity of vortex shedding characterized by C'_L is responsible for the drag augmentation. Lift and drag are determined by integration of pressure and wall shear stress along the airfoil surface. Discrepancies to the experiments basically arise from occurring three-dimensional effects due to the sidewalls in the experiments, which are neglected in the computations.

Besides the mean quantities, the computational results also provide the unsteady behavior of the entire flowfield and especially the structures of the flow behind the Gurney flap (Fig. 22a). Figure 22 shows isocontours of λ_2, the second largest eigenvalue of a combination $S_{ik}S_{kj} + \Omega_{ik}\Omega_{kj}$ of the strain and vorticity tensors. All negative isocontours of λ_2 include a local minimum of pressure and can, therefore, be used to identify vortices in complex flows.[29]

Table 6 Computed integral quantities and dominant frequency for $\alpha = 0$ deg and varying flap height[a]

h_{GF}/c	$\overline{C_L}$	C'_L	$\overline{C_D}$	Sr
Clean	0.636	0.000	0.008	0.12
0.5	0.709	0.000	0.008	0.10
1.0	0.855	0.004	0.011	0.11
1.5	0.957	0.014	0.016	0.15
2.0	1.035	0.017	0.022	0.16

[a]Airfoil HQ17.

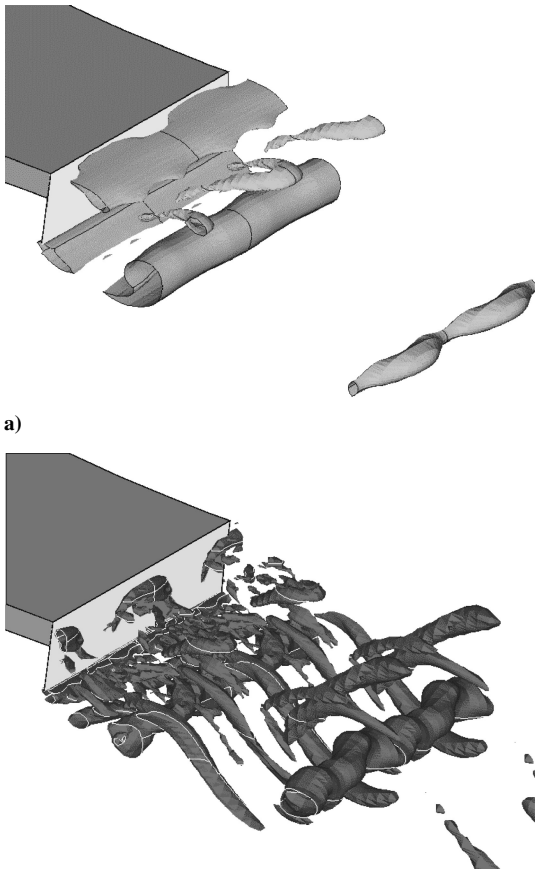

a)

b)

Fig. 22 Isosurfaces of λ_2 in the wake of two-dimensional Gurney flap with $h_{GF}/c = 1\%$ computed by a) URANS and b) DES.

One single principal behavior can be observed for each flap height: Two shear layers appear that continuously separate from the top and the bottom end of the flap. After a short distance, they roll up forming alternating vortices of counteracting direction of rotation, which indicates the absolute instability. Although the size of typical structures depends on the flap height, the relation is not proportional; the vortices grow slower. The shape of the occurring flow structures is comparable to particle image velocimetry measurements for a Gurney flap in ground effect by Zerihan and Zhang.[28]

Although snapshots from URANS computations show three-dimensional effects, especially in the near wake behind the suction side, the overall flowfield is characterized by the shedding of two-dimensional rolls (Fig. 22a). The typical behavior of DES is caused by the resolution of turbulent fluctuations in the LES region. Such very complex structures appear in the near wake (Fig. 22b). Compared to URANS, stronger vortices occur, but these are no longer concentrated in a single dominating structure. The prediction of characteristic frequencies compared to experiments can be improved by DES.

B. Slitted (Three-Dimensional) Gurney Flaps

In the experiments, three dimensionally modified Gurney flaps have been shown to reduce the drag. Because computational simulations of such configurations require a considerable numerical effort, only one selected version of slitted Gurney flaps is investigated here. In Fig. 23, the flowfields predicted by URANS and DES are shown. Compared to the Gurney flap without slits, the two-dimensional rolls are weakened and irregular vortices appear instead. Even though in both the URANS and the DES results very complex structures dominate the near wake and in particular the region downstream of the slits, vortex shedding is still visible. Again the intensity of vortices predicted by DES is larger than in the case of URANS. Compared to the strong rolls behind the two-dimensional Gurney flap, here

Table 7 Integral quantities and Strouhal number for two- and three-dimensional Gurney flaps computed by DES: $\alpha = 0$ deg, $Re = 1 \times 10^6$[a]

Configuration	$\bar{C}_l$	C_l'	$\bar{C}_d$	Sr
Experiment two-dimensional Gurney flap	0.851	——	0.016	0.14
DES two-dimensional Gurney flap	0.823	0.004	0.012	0.13
Experiment three-dimensional Gurney flap	0.813	——	0.015	——
DES three-dimensional Gurney flap	0.810	0.014	0.012	0.12

[a]Airfoil HQ17.

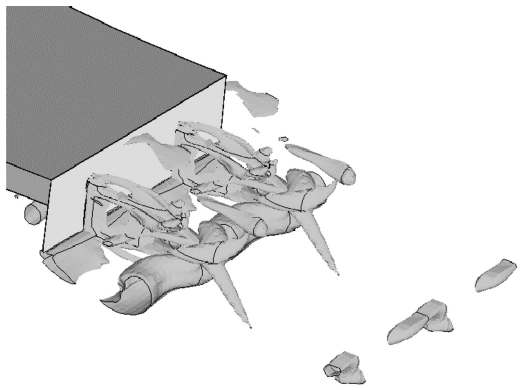

a)

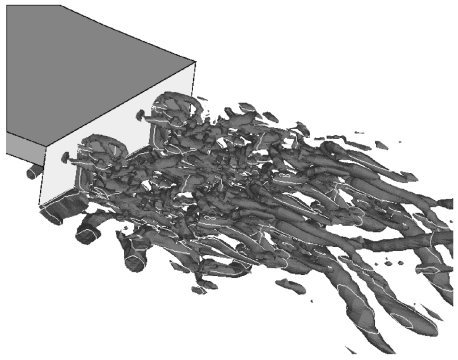

b)

Fig. 23 Isosurfaces of λ_2 in the wake of three-dimensional Gurney flap with slits computed by a) URANS and b) DES.

the smaller structures with no common orientation tend to interact and dissipate faster. They vanish without being convected far downstream. The main effect of the slits in drag reduction is based on this phenomenon. The introduction of slits leads to a drop in lift of about 5% (Table 7). In the DES, the drag can be reduced similarly to the experiments, predicting a reduction of mean drag by 12% coupled with strong three dimensionality and a significant reduction of lift fluctuation.

V. Summary

The drag reduction produced by three-dimensional Gurney flaps has been shown to be effective with the investigated airfoils and the SCCH model. The drag reduction is clearly shown by force measurements. The impact of the three-dimensional modification of the Gurney flaps on the lift is relatively small. The spectrum of the velocity fluctuations shows a discrete frequency with a two-dimensional Gurney flap. When using a three-dimensional Gurney flap, the amplitude of this discrete frequency is clearly reduced. During the current investigations, differences in the effectiveness of the various devices in terms of drag reduction have become clear. On airfoils HQ17 and FX73, the drag reduction is apparent over a larger range of angle of attack. The effective range of the angle of attack of the three-dimensional Gurney flap is substantially smaller on the SCCH model. This is a characteristic of the airfoil, as well as the experimental setup. On the wings in the two-dimensional test section, no or hardly any secondary flows occur on the airfoil. The flow on the SCCH model is distinctly more three dimensional due to the swept wing and the free tip, especially for larger angles of attack. In general, periodic flow separation can be found on wings with an almost two-dimensional flowfield (small or no sweep angle) and an airfoil profile with approximately the same upper and lower boundary-layer thicknesses. This case can be influenced effectively with the three-dimensional Gurney flap configurations.

Unsteady computations show that the Gurney flap enhances the mean lift coefficient similarly to the experimental results. Additionally, a significant augmentation of drag along side the higher lift is closely coupled to the appearance of unsteady two-dimensional flow structures in the wake. The numerical simulations show dominant structures that strongly depend on the flap height. Results that are in satisfying agreement with experiments can be obtained using the LLR k–ω turbulence model, as well as by computations based on a DES. In the case of URANS, very regular structures appear in the wake, whereas the DES predicts more complex flow structures, which are nevertheless dominated by the same vortex-shedding mechanism. Three-dimensional slits in the Gurney flaps do disturb the two dimensionality of the wake and reduce the drag by 12% in the present computation.

Acknowledgment

This research has been funded by the German National Science Foundation under the umbrella of the Special Research Activity (Sonderforschungsbereich) SFB 557, Beeinflussung komplexer turbulenter Scherströmungen at Technical University of Berlin.

References

[1]Gruschwitz, E., and Schrenk, O., "Über eine einfache Möglichkeit zur Auftriebserhöhung von Tragflügeln," *Zeitschrift für Flugtechnik und Motorluftschiffahrt*, Vol. 20, Oct. 1932, pp. 597–601.

[2]Abbott, I. H., and von Doenhoff, A. E., *Therory of Wing Sections*, Dover, New York, 1959, Chap. 8.

[3]Zaparka, E. F., "Aircraft and Control Thereof," U.S. Patent No. 19,412, Jan. 1935.

[4]Liebeck, R. H., "Design of Subsonic Airfoils for High Lift," *Journal of Aircraft*, Vol. 15, No. 9, 1978, pp. 547–561.

[5]Ross, J. C., Storms, B. L., and Carrannanto, P. G., "Lift-Enhancing Tabs on Multielement Airfoils," *Journal of Aircraft*, Vol. 32, No. 3, 1995, pp. 649–655.

[6]Storms, B. L., and Ross, J. C., "Experimental Study of Lift-Enhancing Tabs on a Two-Element Airfoil," *Journal of Aircraft*, Vol. 32, No. 5, 1995, pp. 1072–1078.

[7]Henne, P. A., "Innovation with Computational Aerodynamics: The Divergent Trailing-Edge Airfoil," *Applied Computational Aerodynamics*, edited by P. A. Henne, Vol. 125, Progress in Aeronautics, AIAA, Washington, DC, 1990, Chap. 8.

[8]"Boeing Studying 747 Variants," *Aviation Week and Space Technology*, 28 June 1999, p. 71.

[9]Bechert, D. W., Stanewsky, E., and Hage, W., "Windkanalmessungen an einem Transsonik-Flügel mit strömungsbeeinflussenden Maßnahmen. Teil I: Polaren," DLR, German Aerospace Center, Internal Rept. DLR-IB 92517-99/B3-1, Berlin/Goettingen, June 1999.

[10]Bechert, D. W., Stanewsky, E., and Hage, W., "Windkanalmessungen an einem Transsonik-Flügel mit strömungsbeeinflussenden Maßnahmen. Teil II: Druckverteilungen," DLR, German Aerospace Center, Internal Rept. DLR-IB 92517-99/B3-2, Berlin/Goettingen, June 1999.

[11]Sauvage, P., "Étude expérimentale et numérique des écoulements potentiels et visqueux dans le voisinage d'un bord de fuite épais cambré," Ph.D. Dissertation, L'École Nationale Supérieure de l'Aéronautique et de l'Espace, Toulouse, No. d'ordre: 237, Feb. 1998.

[12]Kentfield, J. A. C., "Theoretically and Experimentally Obtained Performances of Gurney Flap Equipped Wind Turbines," *Wind Engineering*, Vol. 18, No. 2, 1994, pp. 63–74.

[13]Sauvage, P., Pailhas, G., and Coustols, E., "Detailed Flow Pattern Around Thick Cambered Trailing Edges," 7th Asian Congress of Fluid Mechanics, Dec. 1997.

[14]Lee, H. T., and Kroo, I. M., "Computational Investigation of Wings with Miniature Trailing Edge Control Surfaces," AIAA Paper 2004-2693, June 2004.

[15]Schatz, M., Günther, B., and Thiele, F., "Computational Modeling of the Unsteady Wake Behind Gurney Flaps," AIAA Paper 2004-2417, June 2004.

[16]Roshko, A. B., "Bluff Bodies," *Journal of Aeronautical Sciences*, 1955, p. 124.

[17]Bechert, D. W., Meyer, R., and Hage, W., "Drag Reduction of Airfoils with Miniflaps. Can We Learn from Dragonflies?," AIAA Paper 2000-2315, June 2000.

[18]Meyer, R., Bechert, D. W., and Hage, W., "Drag Reduction on Gurney Flaps and Diverging Trailing Edges," *Notes on Numerical Fluid Mechanics*, Vol. 76, Springer-Verlag, Berlin, 2000, pp. 229–245.

[19]Jeffrey, D., Zhang, X., and Hurst, D. W., "Aerodynamics of Gurney flaps on a Single-Element High-Lift Wing," *Journal of Aircraft*, Vol. 37, No. 2, 2000, pp. 295–301.

[20]Hoerner, S. F., *Fluid Dynamic Drag*, published by author, Midland Park, NJ, 1965.

[21]Allen, J. B., "Trailing edge Splitter," U.S. Patent No. 5,265,830, 30 Nov. 1993.

[22]Meyer, R., "Experimentelle Untersuchungen von Rückstromklappen auf Tragflügeln zur Beeinflussung von Strömungsablösungen," Ph.D. Dissertation, Hermann-Foettinger Inst. for Fluid Dynamics, Technical Univ. Berlin, Berlin, Dec. 2000.

[23]Bechert, D. W., "Excitation of Instability Waves," *Zeitschrift für Flugwissenschaften und Weltraumforschung*, Vol. 9, No. 6, 1985, pp. 356–361.

[24]Huerre, P., and Monkewitz, P., "Absolute and Convective Instabilities in Free Shear Layers," *Journal of Fluid Mechanics*, Vol. 159. 1985, pp. 151–168.

[25]Koch, W., "Local Instability Characteristics and Frequency Determination of Self-Excited Wake Flows," *Journal of Sound and Vibration*, Vol. 99, No. 1, 1985, pp. 53–83.

[26]Rung, T., and Thiele, F., "Computational Modelling of Complex Boundary-Layer Flows," *9th International Symposium on Transport Phenomena in Thermal–Fluid Engineering*, 1996, pp. 321–326.

[27]Schatz, M., "Numerische Simulation der Beeinflussung instationärer Strömungsablösung durch frei bewegliche Rückstromklappen auf Tragflügeln," Ph.D. Dissertation, Hermann-Foettinger Inst. for Fluid Dynamics, Technical Univ. Berlin, Berlin, June 2003.

[28]Zerihan, J., and Zhang, X., "Aerodynamics of Gurney Flaps on a Wing in Ground Effect," *AIAA Journal*, Vol. 39, No. 5, 2001, pp. 772–780.

[29]Jeong, J., and Hussain, F., "On the Identification of a Vortex," *Journal of Fluid Mechanics*, Vol. 285, 1995, pp. 69–94.